



## Rigid folding analysis of offset crease thick folding

Jason S. Ku, Erik D. Demaine

MIT Computer Science and Artificial Intelligence Laboratory  
32 Vassar Street, Cambridge, Massachusetts 02139 USA  
jasonku@mit.edu, edemaine@mit.edu

### Abstract

The offset crease method is a procedure for modifying flat-foldable crease patterns in order to accommodate material thickness at creases. This paper analyzes the kinematic configuration space for the family of non-spherical linkage constructed by applying the offset crease method. We provide the system of equations that describes the parameterized configuration space of the linkage, and we visualize the two-dimensional solution space using appropriate projections onto the five-dimensional state space. By analyzing the projections over the space of flat-foldable crease patterns, we provide evidence that the flat and fully-folded states generated by the offset crease method are connected in the configuration space. We also present software for designing and constructing modified crease patterns using the offset crease method.

**Keywords:** folding, origami, thickness, rigid folding, configuration space

### 1. Introduction

Folding is a natural paradigm for manufacturing and designing shell and spatial structures. A significant body of existing research studies the design of flat foldings from perfectly thin, zero-thickness sheets. Such flat foldings are of particular interest due to their analysis simplicity, compactness, and deployability. However, such results are often not applicable when designing structures that must be built using physical materials where the volume of the surface cannot safely be ignored. For example, when designing a complex electric circuit with many layers of components folded on top of one another, the components and the substrate on which they reside have thickness that must be considered and aligned. At a larger scale, architectural and astronomical folded structures made of thick structural materials must be handled.

Over the past few years, a number of approaches have been developed to apply the research of 2D flat foldings to 3D materials, each with their own strengths and weaknesses. In 2015, the authors presented a new offset crease method for creating thick versions of flat foldable crease patterns that preserves the structure of the original crease pattern, replacing each crease with two parallel creases separated by a designated crease width, resulting in a structure whose facets are separated from one another in the final folded state [3]. This replacement creates difficulties at crease intersections since the offset creases will no longer converge to a point. Material in the vicinity around each crease pattern vertex is thus discarded to accommodate crease thickening. While this modification creates holes in the material, it introduces extra degrees of freedom that can allow the thickened creases to fold.

While this construction guarantees both the unfolded and completely folded states of the generated

crease pattern, these two states do not guarantee a rigid folding motion linking the two states, even if the original input crease pattern can fold rigidly. This paper investigates the conditions under which rigid folding can occur for foldings generated by the offset crease method. We analyze the configuration space of four crease vertices thickened using the offset crease method, show that it is set of 2D surfaces, and explore the space analytically and numerically. Non-spherical linkages are generally characterized by equations that cannot be solved fully analytically. Some recent work by Chen et al. studies special cases of a specific class of non-spherical linkage [1]. Our approach is to formulate the closure constraint described by [5], simplify the set of equations, and analyze their properties. In the following sections, we derive the system of equations that describes the parameterized configuration space of the linkage formed by a four-crease, flat-foldable, single-vertex crease pattern, and we visualize the two-dimensional solution space using appropriate projections onto the five-dimensional state space. By analyzing the projections over the space of flat-foldable crease patterns, we provide evidence that the flat and fully-folded states generated by the offset crease method are connected in the configuration space.

In addition, we present software that may be used to design and generate thick foldings using the offset crease technique. The software allows the user to import their own flat foldable crease patterns and generate thickened versions of them interactively via an online web application. We comment on the usage and development of this software.

## 2. Theory

In this section, we compare the kinematics of flat-foldable, single-vertex crease patterns having exactly four creases, with thickened versions of the crease patterns constructed using the offset crease method.

Consider a unit circle of paper with four straight line creases emanating from the center of the paper that satisfies Kawasaki's local flat foldability condition: the alternating sum of the cyclically ordered sector angles formed by the creases is zero. We will call the smallest sector angle  $\alpha$  and let  $\beta$  be a sector angle adjacent to  $\beta$  with  $0 < \alpha \leq \beta \leq \pi$ . Choosing  $\beta$  from the range  $(0, \pi)$  and  $\alpha$  from the range  $(0, \min(\beta, \pi - \beta)]$  parameterizes all non-degenerate four-crease, flat-foldable, single-vertex crease patterns.

Number the creases such that angle  $\alpha$  is bounded by creases  $c_1$  and  $c_2$ , angle  $\beta$  is bounded by creases  $c_2$  and  $c_3$ , with crease  $c_4$  opposite  $c_1$ . Let  $u_i$  be the unit vector aligned with crease  $c_i$ . Also let  $\theta_i$  be the sector angle between creases  $c_i$  and  $c_{i+1}$ , with the convention that  $i + 1$  and  $i - 1$  represent the next and previous indices in the cyclic order. In this section, index arithmetic will always be taken modulo 4.

We now model rigid folded states of the crease pattern. The kinematics of four-crease, flat-foldable, single-vertex crease patterns is well studied [2][4]. To fold the crease pattern, paper facets rotate rigidly around the creases. Let the turn angle  $\phi_i$  be the angular deviation of the faces bounding crease  $c_i$ , with positive turn angle consistent with a right handed rotation around direction of the crease. A four crease vertex has a single degree of freedom which may be parameterized by the turn angle  $\rho$  of one crease. Let  $\rho$  equal  $\phi_1$ . In a rigid folding of the vertex, the turn angle at one of the creases bounding the smallest angle  $\alpha$  must have sign opposite from the other three angles [2]. Without loss of generality, assume  $c_2$  has opposite sign. Then the turn angles at the other creases are  $\phi_3 = \phi_1$  and

$$-\phi_2 = \phi_4 = \arccos\left(\cos \rho + \frac{\sin^2 \rho}{\cos \rho + \cot \alpha \cot \beta + \csc \alpha \csc \beta}\right) \quad (1)$$

It will be useful to attach a local coordinate frames in order to relate different parts of the paper. See Figure 1. When the paper is flat, we define a local coordinate frame relative to each crease, with  $u_i$  being the unit vector in the direction of crease  $c_i$ , and  $t_i$  being the unit vector orthogonal to  $u_i$  taken

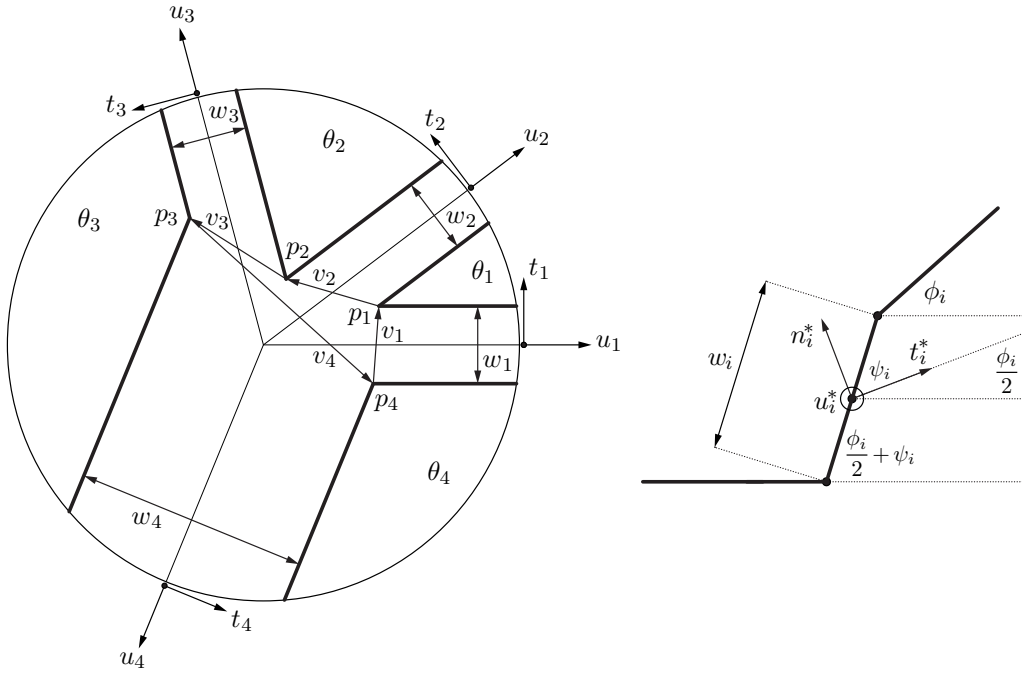


Figure 1: Diagrams showing a linkage constructed by applying the offset crease method to a generic four-crease, flat-foldable, single-vertex crease pattern. [Left] The crease pattern in its flat state, with sector angles  $\theta_i$  and crease widths  $w_i$ . Local flat coordinate frames  $(u_i, t_i)$  are also shown, as are the vectors  $v_i$  from point  $p_{i-1}$  to point  $p_i$ . [Right] A local cross section looking down a crease during folding with unit vector  $u_i^*$  pointing out of the page.

counter clockwise. When the paper is being folded, we will define more local coordinate frames, this time moving with each crease. Unit vector  $u_i^*$  will be in the direction of crease  $c_i$  during folding,  $n_i^*$  will be the average of the normal vectors of the faces adjacent to  $c_i$ , and  $t_i^*$  will be the transverse direction such that  $u_i^* \times t_i^* = n_i^*$ . Instead of relating these frames to some fixed coordinate system, we will instead write our equations in terms of dot products between these vectors which will be agnostic to any specific embedding.

Let us now widen each crease using the offset crease method. Let  $w_i$  be the width ascribed to crease  $c_i$ . The offset crease method requires that  $w_4$ , the width of the external crease, equals the sum of the other three widths, so that  $w_4 = w_1 + w_2 + w_3$ . We construct points  $p_i$  defining the intersections of the offset creases so that each  $p_i$  is distance  $w_i/2$  from crease  $c_i$  and distance  $w_{i+1}/2$  from crease  $c_{i+1}$ . Of particular interest are the vectors  $v_i = p_i - p_{i-1}$  running from  $p_{i-1}$  to  $p_i$ , because summing these vectors defines a closure constraint that must sum to zero during folding. Note that the dot product of  $v_i$  with respect to the flat coordinate frame associated with crease  $c_i$  is:

$$v_i \cdot \begin{bmatrix} t_i \\ u_i \end{bmatrix} = \begin{bmatrix} w_i \\ \frac{1}{2} \left( \frac{w_i \cos \theta_i + w_{i+1}}{\sin \theta_i} - \frac{w_i \cos \theta_{i-1} + w_{i-1}}{\sin \theta_{i-1}} \right) \end{bmatrix}. \quad (2)$$

Now let  $v_i^*$  be the direction of  $v_i$  during a folding motion. Splitting each crease into two creases means that when the crease pattern folds, the turn angle  $\phi_i$  at crease  $c_i$  must then be split between two creases. Choosing  $n_i^*$  to be the average of adjacent face normals means if  $v_i^*$  is perpendicular to  $n_i^*$ , the turn angle will be split evenly between the two split creases. Otherwise, the face created at the widened crease could rotate around  $u_i^*$  with an additional rotational degree of freedom. We call this rotation *split angle*  $\psi_i$ ,

such that:

$$v_i^* = (v_i \cdot u_i)u_i^* + (v_i \cdot t_i)(\cos(\psi_i)t_i^* + \sin(\psi_i)n_i^*). \quad (3)$$

Then the solution space of folded isometries of the thickened flat-foldable four-crease vertex is given by the following closure constraint:

$$0 = \sum_{i=1}^4 v_i^* \quad (4)$$

Projected onto any generic fixed reference frame, this vector equation yields three equations, with each dependent on all four unknowns  $\psi_i$  for all  $i \in \{1, 2, 3, 4\}$ . However, we notice that projecting the equation in the direction of a crease  $u_i^*$ , we get an equation in only three variables as  $\psi_i$  drops out since  $t_i^* \cdot u_i^* = n_i^* \cdot u_i^* = 0$ :

$$0 = \sum_{i=1}^4 (v_i \cdot u_i)(u_i^* \cdot u_j^*) + (v_i \cdot t_i) (\cos(\psi_i)(t_i^* \cdot u_j^*) + \sin(\psi_i)(n_i^* \cdot u_j^*)) \quad (5)$$

As long as the no two creases are collinear in the original crease pattern which would lead to a degenerate folding motion, choosing Equation 5 for any three  $j$  in  $\{1, 2, 3, 4\}$  will yield three independent equations in four unknowns, except that each of the equations will only contain three of the unknowns. Below are explicit values for the dot products needed:

$$u_i^* \cdot \begin{bmatrix} u_i^* \\ u_{i+1}^* \\ u_{i+2}^* \\ u_{i+3}^* \end{bmatrix} = \begin{bmatrix} 1 \\ \cos \theta_i \\ \cos \theta_i \cos \theta_{i+1} - \sin \theta_i \sin \theta_{i+1} \cos \phi_{i+1} \\ \cos \theta_{i-1} \end{bmatrix} \quad (6)$$

$$u_i^* \cdot \begin{bmatrix} t_i^* \\ t_{i+1}^* \\ t_{i+2}^* \\ t_{i+3}^* \end{bmatrix} = \begin{bmatrix} 0 \\ -\sin \theta_i \cos \frac{\phi_{i+1}}{2} \\ -(\sin \theta_{i+1} \cos \theta_i + \cos \theta_{i+1} \sin \theta_i \cos \phi_{i+1}) \cos \frac{\phi_{i+2}}{2} + \sin \theta_i \sin \phi_{i+1} \sin \frac{\phi_{i+2}}{2} \\ \sin \theta_{i-1} \cos \frac{\phi_{i-1}}{2} \end{bmatrix} \quad (7)$$

$$u_i^* \cdot \begin{bmatrix} n_i^* \\ n_{i+1}^* \\ n_{i+2}^* \\ n_{i+3}^* \end{bmatrix} = \begin{bmatrix} 0 \\ \sin \theta_i \sin \frac{\phi_{i+1}}{2} \\ (\sin \theta_{i+1} \cos \theta_i + \cos \theta_{i+1} \sin \theta_i \cos \phi_{i+1}) \sin \frac{\phi_{i+2}}{2} + \sin \theta_i \sin \phi_{i+1} \cos \frac{\phi_{i+2}}{2} \\ \sin \theta_{i-1} \sin \frac{\phi_{i-1}}{2} \end{bmatrix} \quad (8)$$

For example, for  $j = 1$ , Equation 5 evaluates to Equation 9 below. This equation has a particularly nice form.

$$\begin{aligned} 0 = & \frac{1}{2} (w_2 \sin \theta_1 + w_4 \sin \theta_4 + w_3 \sin(\theta_1 + \theta_2)) + \\ & \frac{1}{2} \sin \theta_1 \cos \phi_2 (w_2 + w_3 (\cos \theta_2 - \sin \theta_2 \cot \theta_3) - w_4 \sin \theta_2 \csc \theta_3) - \\ & w_2 \sin \theta_1 \cos \left( \psi_2 + \frac{\phi_2}{2} \right) + w_4 \sin \theta_4 \cos \left( \psi_4 - \frac{\phi_4}{2} \right) + \\ & w_3 \left( \sin \theta_1 \sin \phi_2 \sin \left( \psi_3 + \frac{\phi_3}{2} \right) - (\cos \theta_1 \sin \theta_2 + \sin \theta_1 \cos \theta_2 \cos \phi_2) \cos \left( \psi_3 + \frac{\phi_3}{2} \right) \right). \end{aligned} \quad (9)$$

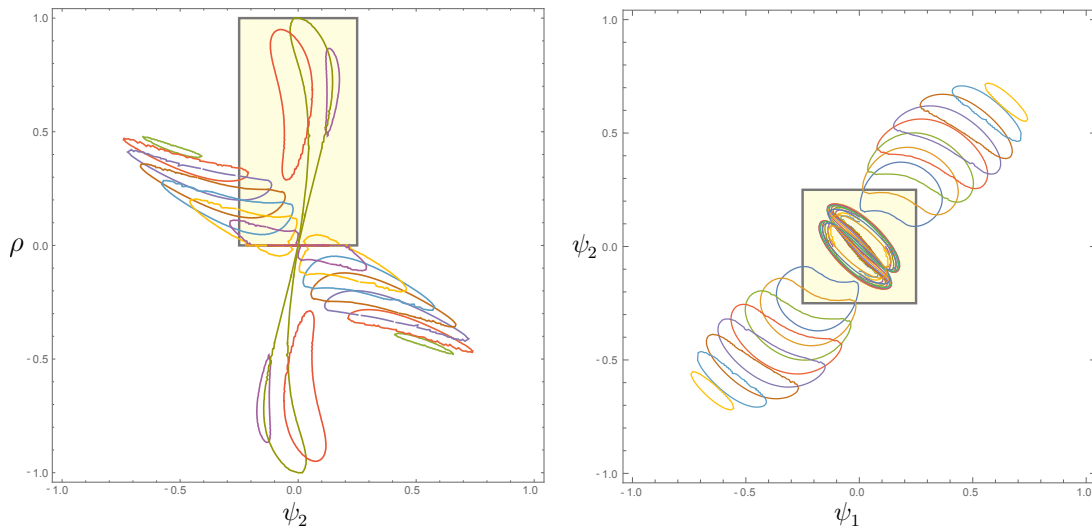


Figure 2: Two projections of the configuration space for a fixed offset crease pattern with  $\alpha = \pi/8$  and  $\beta = \pi/2$ . [Left] Projection onto  $\rho$  and  $\psi_2$  showing curves of constant  $\psi_1$ . [Right] Projection onto  $\psi_1$  and  $\psi_2$  showing curves of constant  $\rho$ . The yellow region encloses the primary lobe which is highlighted in more detail in Figure 3.

The other four equations have the same form, and can be obtained by permuting the indices. This technique, formulating a vector closure condition and then projecting in directions that reduce variables is a general technique that can be applied to the analysis of higher degree vertices. By combining equations of this form, we can obtain a scalar equation in terms of the parameters of the problem and our choice of any two split angles, for example  $\psi_1$  and  $\psi_2$ . Combined with the fold angle  $\rho$ , we have one constraint in three unknowns yielding generically an algebraic manifold with a two-dimensional intrinsic dimension, and we expect the folding to have locally two degrees of freedom.

### 3. Analysis

Now let us visualize the configuration space for a specific crease pattern. We parameterize our test case with  $\alpha = \pi/8$ ,  $\beta = \pi/2$ ,  $w_1 = w_2 = w_3 = 1$ , and  $w_4 = 3$ . The left of Figure 2 shows a projection of the configuration space onto the  $\psi_2 \times \rho$  torus, plotting contour lines for a range of fixed values of  $\psi_1$  between  $\pm\pi$  at intervals of  $\pi/10$ , while the right shows a projection onto the  $\psi_1 \times \psi_2$  torus, plotting contour lines for values of  $\rho$  between 0 and  $\pi$  at intervals of  $\pi/20$ . On the left, the center point represents the flat folded state having zero fold angle with all split angles  $\psi_i$  fixed to zero. The configuration space is rotationally symmetric around the center since our analysis is agnostic to our choice of crease pattern orientation. The top center (and bottom center) of the plot represents the fully folded state guaranteed by the offset-crease construction. It is the tear-dropped section of the configuration space connecting that top and bottom that we are interested in. We will call this section the *primary lobe*, with the other section being the *secondary lobe*.

We comment here briefly on the other sections of the configuration space. The lobes to the left and right of the primary lobe corresponds to another folding mode in which split angles deviate quickly away from zero. In this instance, they connect to the primary lobe only at the flat configuration. When this happens, the folding is unable to fold fully to the  $180^\circ$  fold angle because the faces translate dramatically relative to the original folding motion.

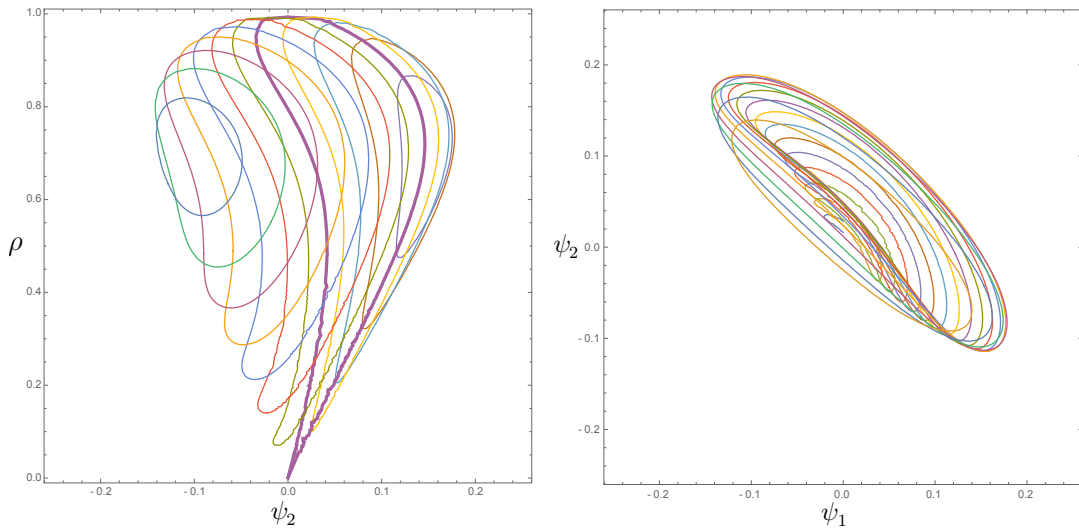


Figure 3: Two projections of the primary lobe, a subset of the configuration space for a fixed offset crease pattern with  $\alpha = \pi/8$  and  $\beta = \pi/2$ . [Left] Projection onto  $\rho$  and  $\psi_2$  showing curves of constant  $\psi_1$ . [Right] Projection onto  $\psi_1$  and  $\psi_2$  showing curves of constant  $\rho$ .

Figure 3 shows detail of the primary lobe at higher resolution. Observe that the configuration space of the primary lobe for this crease pattern is a topological 2-sphere, with what seems to be a single not smooth point at the flat configuration. So for this crease pattern, the flat and folded states of the modified crease pattern are in fact connected in the configuration space by a continuum of paths around this sphere. In fact, if we observe the purple contour line with fixed  $\psi_1 = 0$  extending from the bottom point, we can observe that this curve represents two specific paths through the configuration space connecting the two points.

The goal now is to see if such a path exists for any four-crease, flat-foldable, single-vertex crease pattern, not just for this specific instance. Figure 4 plots projections of the configuration space for different crease patterns. The horizontal distribution of the plots varies with the parameter  $\beta$  for values evenly spanning the range  $(0, \pi)$ , while the vertical distribution varies with parameter  $\alpha$  spanning the range  $(0, \min(\beta, \pi - \beta))$ . Each curve represents a subset of the configuration space restricted to one split angle being zero,  $\psi_i = 0$ , projected onto the torus spanning  $\rho$ , on the horizontal axes ranging from  $-\pi$  to  $\pi$ , and  $\psi_j$ , on the vertical axes ranging from 0 to  $\pi$ . The color of the curves correspond to which values of  $i$  and  $j$  are shown.

Looking over the range of possible values, we can make the following observations. First, we observe that for some crease patterns, the primary and secondary lobes merge into a single connected component, specifically for  $\beta \geq \pi/2$  and sufficiently large  $\alpha$ . This feature be seen particularly in the blue, yellow, and green curves corresponding respectively to zeroing split angles associated with creases  $c_1$ ,  $c_2$ , and  $c_3$ . In particular, when fixing the split angle associated with any of these three angles, a path exists between the flat and folded states that monotonically increases in  $\rho$ , though more complicated paths also exists that do not increase monotonically in  $\rho$ .

However, observe that if the split angle of the external crease  $c_4$  is fixed at zero, the configuration space becomes disconnected for crease patterns with  $\alpha$  sufficiently small. This feature can be seen in the red circular components that are incident to the fully-folded state, but not to the flat state. Thus, we cannot always achieve a folding motion by fixing the split angle at any crease to zero; a path may not exist for some crease patterns when the external crease split angle is fixed.

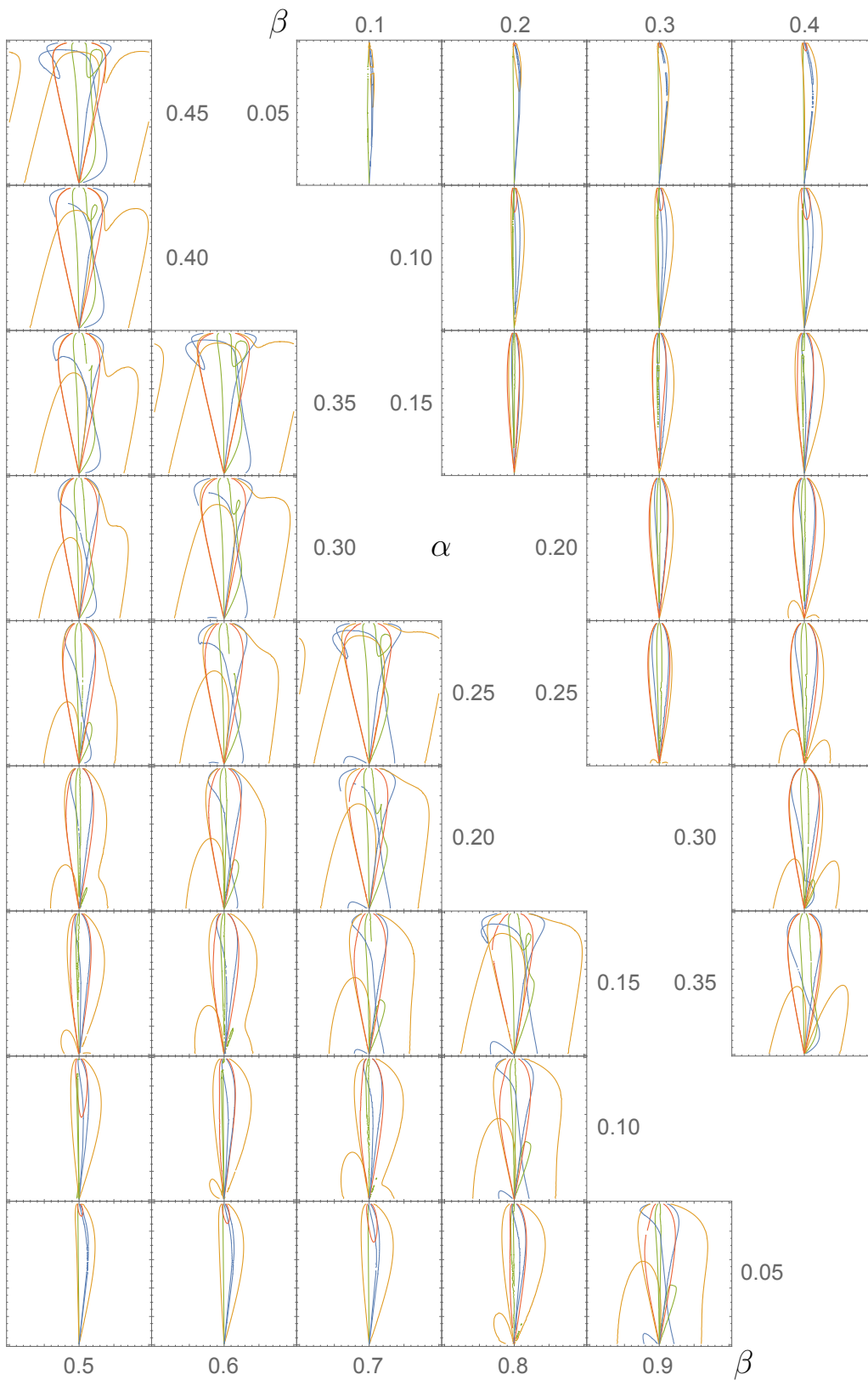


Figure 4: Projections of the configuration space for fixed values of  $\psi_i$ , for different flat-foldable creases patterns parameterized by  $\alpha$  and  $\beta$  in fractions of  $\pi$ . Each curve represents a subset of the configuration space restricting  $\psi_i = 0$ , projected onto  $\rho$  (horizontal ranging from  $-\pi$  to  $\pi$ ) and  $\psi_j$  (vertical ranging from  $0$  to  $\pi$ ). The colors [blue, yellow, green, red] correspond to  $(i, j) = [(1, 2), (2, 3), (3, 4), (4, 1)]$  respectively.

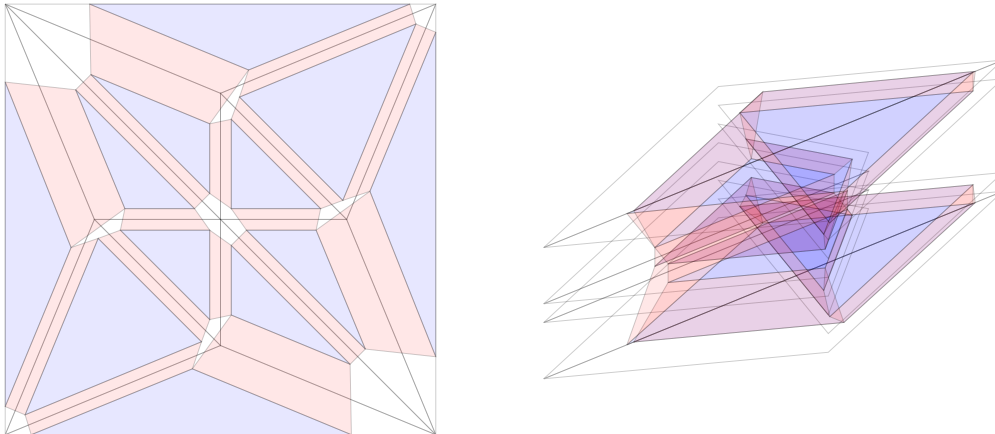


Figure 5: A screenshot of our offset crease implementation in action. The model shown is a traditional bird base with uniform thickness offset.

#### 4. Software

We wrote a program to implement the algorithm presented in [3] for generating modified offset crease patterns from input flat-foldable crease patterns. The program was written in coffeescript and can be found at <http://jasonku.scripts.mit.edu/thick>. The input is a vertex set and an ordered list of faces. The program allows the user to adjust the distance between faces by pressing arrow keys, allowing the user to view how the crease pattern changes in real time. Figure 5 shows a screen shot of the implementation. For more details and access to the source, please contact the corresponding author.

#### 5. Conclusion

This paper has provided a general technique for analyzing the configuration space for non-spherical linkages by visualizing projections of the state space, and has applied this technique to study the configuration space for single vertex crease patterns generated by the offset crease method. We have provided evidence to support that there always exist a path between the flat and fully-folded states guaranteed by the offset crease method construction. Future work is needed in order to extend this analysis to higher degree vertices. Further, our analysis does not forbid local binding between adjacent faces, so additional work would be needed to characterize if and when binding could occur.

#### References

- [1] Yan Chen, Rui Peng, and Zhong You. Origami of thick panels. *Science*, 349(6246):396–400, 2015.
- [2] David A. Huffman. Curvature and creases: A primer on paper. *IEEE Trans. Computers*, 25(10):1010–1019, 1976.
- [3] Jason S. Ku and Erik D. Demaine. Folding flat crease patterns with thick materials. *Journal of Mechanisms and Robotics*, 8(3):031003–1–6, June 2016.
- [4] Robert J Lang, Spencer Magleby, and Larry Howell. Single degree-of-freedom rigidly foldable cut origami flashers. *Journal of Mechanisms and Robotics*, 8(3):031005, 2016.
- [5] sarah-marie belcastro and Thomas C. Hull. Modelling the folding of paper into three dimensions using affine transformations. *Linear Algebra and its Applications*, 348(13):273 – 282, 2002.